Proceedings of ALGORITMY 2016
pp. 103–112

ON A NEW APPROACH TO 3D MESHLESS FLOWS SIMULATION AROUND BLUFF BODIES BY USING VORTEX METHOD*

ILIA K. MARCHEVSKY† AND GEORGY A. SHCHEGLOV‡

Abstract. The original approach is suggested for vortex sheet intensity computation when 3D flow around bluff bodies is being simulated using meshless Lagrangian vortex methods. Integral equation approximate solution is based on its approximation by the system of linear algebraic equations, which coefficients are expressed through improper integrals. In order to compute these integrals the numerical scheme is developed which allows to exclude the singularities, i.e., to split the integrals into regular and singular parts. Regular parts can be integrated numerically with high precision by using Gaussian quadrature formulae and for singular parts exact analytical expressions are derived.

The developed approach allows to raise significantly the accuracy of vortex method. It is shown that the developed semi-analytical procedure of integrals computation is much more accurate in comparison with direct numerical integration. The test problem of flow simulation around the sphere is considered. The exact analytical solution is known for it, and the developed approach provides more accurate results in comparison with 'classical' 3D vortex method, especially when non-uniform unstructured triangular meshes are used for bodies surface representation.

Key words. vortex element method, vorticity flux, integral equation, quadrature formula, singularity exclusion, flow simulation

AMS subject classifications. 76M23, 45E05, 65R20

1. Introduction.

Vortex element method (VEM) is very suitable when solving fluid-structure interaction (FSI) problems, especially two-way coupled hydroelastic problems, when it is important to simulate unsteady body motion in incompressible flow [1]. Pure Lagrangian modifications of vortex methods don't require mesh generation in the fluid domain and its reconstruction at every time step due to body's motion. Vortex methods need much less computational resources (time of computations, memory and disk space) in comparison with most popular mesh methods.

Flow simulation using VEM requires the solution of two main problems: vortex wake evolution simulation and vorticity flux on the body surface computation, which are solved sequentially, step by step at every time step. In order to simulate vortex wake evolution there are developed number of approaches: vortex wake approximation with vortex filaments, vortex lattices, vortex points (vortons) of different types etc. The vortex fragmenton model is developed by authors and it has been applied to some FSI-problems [2]. As to vorticity flux simulation, one of the most important problems is vortex sheet intensity computation on the body's surface. There are two fundamental approaches, which are based on elimination of the limit values of normal or tangential velocity components on the body surface, respectively [3].

The accuracy of 'normal' approach in some FSI-applications is not enough for practice. In 2D-case 'tangent' approach allows to obtain much more accurate results, but it requires more accurate discretization and precise integration schemes usage [3]. Such schemes are constructed and investigated by authors for 2D-case [4].

*This work was supported by Grant No.: MK-7431.2016.8.

†Applied Mathematics Department, Bauman Moscow State Technical University, Russia, 105005, Moscow, 2-nd Baumanskaya st., 5 (iliamarchevsky@mail.ru).

‡Aerospace Systems Department, Bauman Moscow State Technical University, Russia, 105005, Moscow, 2-nd Baumanskaya st., 5 (shcheglov_ga@mail.ru).

In the present research 3D-case is considered. The discretization scheme for 'tangent' approach is presented. The body surface is triangulated using arbitrary mesh generator and vortex sheet intensity assumed to be piecewise constant over the cells. 'Tangent' approach includes calculation of two surface integrals: the integral over the 'influence' cell and the integral over the 'control' cell. For arbitrary triangular mesh 'influence' integral can be calculated analytically. Numerical calculation of the 'control' integral using Gaussian points leads to significant errors for neighboring cells. In order to solve this problem the specific quadrature formula with analytical singularity exclusion and its analytical integration should be derived. Non-singular part of the integral can be integrated numerically by using Gaussian quadratures.

In the present paper the original algorithm is developed, which is based on the mentioned approach for vortex influences computation. All computation formulae are obtained in invariant form and can be applied for arbitrary triangular cells.

2. Problem statement. The problem of 3D incompressible flow simulation around bluff body is considered. The governing equations are continuity equation and Navier — Stokes equations

$$\nabla \cdot \boldsymbol{V} = 0, \quad \frac{\partial \boldsymbol{V}}{\partial t} + (\boldsymbol{V} \cdot \nabla)\boldsymbol{V} = \nu \nabla^2 \boldsymbol{V} - \frac{\nabla p}{\rho_\infty},$$

with boundary conditions

$$\lim_{r \to \infty} \boldsymbol{V} = \boldsymbol{V}_\infty, \quad \lim_{r \to \infty} p = p_\infty, \quad \boldsymbol{V}(\boldsymbol{r}, t)\Big|_{\boldsymbol{r} \in K} = 0,$$

where $\boldsymbol{V} = \boldsymbol{V}(\boldsymbol{r}, t)$ is flow velocity; $p = p(\boldsymbol{r}, t)$ — pressure; $\rho_\infty = \text{const}$ — density; ν — kinematic viscosity coefficient; $\boldsymbol{V}_\infty$ and p_∞ are parameters of the incident flow; K is body's surface.

The viscosity assumed to be small, so according to L. Prandtl's theory [5] it is possible to take its influence into account only as a cause of vorticity generation on body surface. The flow can be considered inviscid, with vorticity flux from the surface.

The immovable streamlined body is simulated by vortex sheet $\boldsymbol{\gamma}(\boldsymbol{r}, t)$ influence, which is placed on the body surface, $\boldsymbol{r} \in K$. The vorticity flux can be simulated if this vortex sheet is free; that means that at every time step this sheet is split into separate vortex elements which form vortex wake around the body.

Vortex wake evolution can be simulated by using one of Lagrangian vortex element methods [1, 2].

One of the most important problems is vortex sheet intensity computation witch high accuracy. From mathematical point of view it can be done by using one of two equivalent approaches, which are based on elimination of the limit values of normal or tangential velocity components on the body surface [3], hereinafter we call these approaches as 'normal' and 'tangent' ones.

However, 'normal' and 'tangent' approaches are quite different from computational point of view because they lead to numerical solution of integral equations of different types. Numerical experiments show that the accuracy of 'normal' approach sometimes is not enough for practice. 'Tangent' approach is more complicated, but in 2D-case it allows to obtain much more accurate results in comparison with 'normal' one. Numerical schemes for 'tangent' approach in 2D case have been constructed and investigated by authors [4].

The aim of the present research is development of the 'tangent' numerical schemes for 3D incompressible flow simulation around immovable bodies of arbitrary shape.

3. Integral equation for vortex sheet intensity. Due to vortex sheet on the body surface, velocity field has the discontinuity, and its limit value from body side is

$$\overline{\boldsymbol{V}}(\boldsymbol{r},\,t) = \boldsymbol{V}_\infty + \frac{1}{4\pi}\int\limits_{S(t)} \frac{\boldsymbol{\Omega}(\boldsymbol{\xi},\,t)\times(\boldsymbol{r}-\boldsymbol{\xi})}{\left|\boldsymbol{r}-\boldsymbol{\xi}\right|^3}d\xi + \\ + \frac{1}{4\pi}\int\limits_{K} \frac{\boldsymbol{\gamma}(\boldsymbol{\xi},\,t)\times(\boldsymbol{r}-\boldsymbol{\xi})}{\left|\boldsymbol{r}-\boldsymbol{\xi}\right|^3}d\xi - \frac{\boldsymbol{\gamma}(\boldsymbol{r},\,t)\times\boldsymbol{n}(\boldsymbol{r})}{2}, \quad \boldsymbol{r}\in K,$$

where $S(t)$ is vortex wake region; $\boldsymbol{n}(\boldsymbol{r})$ is unit outer normal vector on body surface K.

In order to satisfy the boundary condition on the body surface, vortex sheet intensity should satisfy the integral equation $\overline{\boldsymbol{V}}(\boldsymbol{r},\,t)=0$, $\boldsymbol{r}\in K$.

As it proved in [3], it is enough to satisfy this equation only for tangent component of the velocity:

$$\boldsymbol{n}(\boldsymbol{r})\times\Big(\overline{\boldsymbol{V}}(\boldsymbol{r},\,t)\times\boldsymbol{n}(\boldsymbol{r})\Big)=0.$$

It leads to Fredholm-type integral equation of the 2-nd kind

$$\frac{\boldsymbol{n}(\boldsymbol{r})}{4\pi}\times\left(\int\limits_K \frac{\boldsymbol{\gamma}(\boldsymbol{\xi},\,t)\times(\boldsymbol{r}-\boldsymbol{\xi})}{\left|\boldsymbol{r}-\boldsymbol{\xi}\right|^3}\times\boldsymbol{n}(\boldsymbol{r})d\xi\right) - \frac{\boldsymbol{\gamma}(\boldsymbol{r},\,t)\times\boldsymbol{n}(\boldsymbol{r})}{2} = \boldsymbol{f}(\boldsymbol{r},\,t), \quad \boldsymbol{r}\in K, \tag{3.1}$$

where

$$\boldsymbol{f}(\boldsymbol{r},\,t) = -\boldsymbol{n}(\boldsymbol{r})\times\left[\left(\boldsymbol{V}_\infty + \frac{1}{4\pi}\int\limits_{S(t)}\frac{\boldsymbol{\Omega}(\boldsymbol{\xi},\,t)\times(\boldsymbol{r}-\boldsymbol{\xi})}{\left|\boldsymbol{r}-\boldsymbol{\xi}\right|^3}\,d\xi\right)\times\boldsymbol{n}(\boldsymbol{r})\right]$$

is known vector function.

4. Integral equation discretization. In order to find approximate solution of hypersingular integral equation (3.1), the following assumptions can be made:

1) body surface is triangulated into N flat cells K_i with areas A_i and normal vectors $\boldsymbol{n}_i$, $i=1,\ldots,N$;
2) the unknown vortex sheet intensity on the i-th cell is constant vector $\boldsymbol{\gamma}_i$, $i=1,\ldots,N$, which lies in the plane of the i-th cell, i.e. $\boldsymbol{\gamma}_i\cdot\boldsymbol{n}_i=0$;
3) the integral equation (3.1) is satisfied on average on the cells.

According to these assumptions the discrete analogue of equation (3.1) can be derived:

$$\frac{1}{4\pi A_i}\sum_{j=1}^{N}\int\limits_{K_i}\left(\int\limits_{K_j}\boldsymbol{n}_i\times\left(\frac{\boldsymbol{\gamma}_j\times(\boldsymbol{r}-\boldsymbol{\xi})}{\left|\boldsymbol{r}-\boldsymbol{\xi}\right|^3}\times\boldsymbol{n}_i\right)d\xi\right)dr - \frac{\boldsymbol{\gamma}_i\times\boldsymbol{n}_i}{2} = \\ = \frac{1}{A_i}\int\limits_{K_i}\boldsymbol{f}(\boldsymbol{r},\,t)dr, \quad i=1,\ldots,N. \tag{4.1}$$

To write down (4.1) in form of linear algebraic system we should choose local orthonormal basis on every cell $(\boldsymbol{\tau}_i^{(1)},\,\boldsymbol{\tau}_i^{(2)},\,\boldsymbol{n}_i)$, where tangent vectors $\boldsymbol{\tau}_i^{(1)}$, $\boldsymbol{\tau}_i^{(2)}$ can

be chosen arbitrary and $\boldsymbol{\tau}_i^{(1)} \times \boldsymbol{\tau}_i^{(2)} = \boldsymbol{n}_i$. So $\boldsymbol{\gamma}_i = \gamma_i^{(1)}\boldsymbol{\tau}_i^{(1)} + \gamma_i^{(2)}\boldsymbol{\tau}_i^{(2)}$ and we can project (4.1) for every i-th panel onto the directions $\boldsymbol{\tau}_i^{(1)}$ and $\boldsymbol{\tau}_i^{(2)}$:

$$
\begin{aligned}
&\frac{1}{4\pi A_i}\boldsymbol{\tau}_i^{(1)} \cdot \left(\sum_{\substack{j=1 \\ j\neq i}}^{N} \gamma_j^{(1)}\boldsymbol{\nu}_{ij}^{(1)} + \sum_{\substack{j=1 \\ j\neq i}}^{N} \gamma_j^{(2)}\boldsymbol{\nu}_{ij}^{(2)} \right) - \frac{\gamma_i^{(2)}}{2} = \frac{b_i^{(1)}}{A_i}, \\
&\frac{1}{4\pi A_i}\boldsymbol{\tau}_i^{(2)} \cdot \left(\sum_{\substack{j=1 \\ j\neq i}}^{N} \gamma_j^{(1)}\boldsymbol{\nu}_{ij}^{(1)} + \sum_{\substack{j=1 \\ j\neq i}}^{N} \gamma_j^{(2)}\boldsymbol{\nu}_{ij}^{(2)} \right) + \frac{\gamma_i^{(1)}}{2} = \frac{b_i^{(2)}}{A_i},
\end{aligned}
\tag{4.2}
$$

where

$$
\boldsymbol{\nu}_{ij}^{(k)} = \int\limits_{K_i} \left(\int\limits_{K_j} \frac{\boldsymbol{\tau}_j^{(k)} \times (\boldsymbol{r} - \boldsymbol{\xi})}{\left|\boldsymbol{r} - \boldsymbol{\xi}\right|^3} d\xi \right) dr, \quad b_i^{(k)} = \int\limits_{K_i} \boldsymbol{\tau}_i^{(k)} \cdot \boldsymbol{f}(\boldsymbol{r},\, t)\, dr,
$$

$$
k = 1,\, 2; \quad i, j = 1,\, \ldots,\, N.
$$

Algebraic system (4.2) has infinite set of solutions; in order to select the unique solution we should satisfy additional condition

$$
\int\limits_K \boldsymbol{\gamma}(\boldsymbol{r},\, t)\, dr = \boldsymbol{0},
$$

which can be written down in the following form:

$$
\sum_{i=1}^{N} A_i \left(\gamma_i^{(1)}\boldsymbol{\tau}_i^{(1)} + \gamma_i^{(2)}\boldsymbol{\tau}_i^{(2)} \right) = \boldsymbol{0}. \tag{4.3}
$$

System (4.2)–(4.3) is overdetermined, it should be regularized, for example, by analogy with [6] by introducing the 3D-vector $\boldsymbol{R} = \left(R_1,\, R_2,\, R_3\right)^T$:

$$
\begin{aligned}
&\frac{1}{4\pi A_i}\boldsymbol{\tau}_i^{(1)} \cdot \left(\sum_{\substack{j=1 \\ j\neq i}}^{N} \gamma_j^{(1)}\boldsymbol{\nu}_{ij}^{(1)} + \sum_{\substack{j=1 \\ j\neq i}}^{N} \gamma_j^{(2)}\boldsymbol{\nu}_{ij}^{(2)} \right) - \frac{\gamma_i^{(2)}}{2} + \boldsymbol{R} \cdot \boldsymbol{\tau}_i^{(2)} = \frac{b_i^{(1)}}{A_i}, \\
&\frac{1}{4\pi A_i}\boldsymbol{\tau}_i^{(2)} \cdot \left(\sum_{\substack{j=1 \\ j\neq i}}^{N} \gamma_j^{(1)}\boldsymbol{\nu}_{ij}^{(1)} + \sum_{\substack{j=1 \\ j\neq i}}^{N} \gamma_j^{(2)}\boldsymbol{\nu}_{ij}^{(2)} \right) + \frac{\gamma_i^{(1)}}{2} + \boldsymbol{R} \cdot \boldsymbol{\tau}_i^{(1)} = \frac{b_i^{(2)}}{A_i}, \\
&\sum_{j=1}^{N} A_j \left(\gamma_j^{(1)}\boldsymbol{\tau}_j^{(1)} + \gamma_j^{(2)}\boldsymbol{\tau}_j^{(2)} \right) = 0, \qquad i = 1,\, \ldots,\, N.
\end{aligned}
\tag{4.4}
$$

The dimension of matrix of linear equations system (4.4) is $2N + 3$. Numerical experiments show that this matrix is well-conditioned.

5. Matrix coefficients calculation. The main problem for practical use of the suggested approach is coefficients $\boldsymbol{\nu}_{ij}^{(k)}$ calculation for system (4.4):

$$\boldsymbol{\nu}_{ij}^{(k)} = \int\limits_{K_i} \left(\int\limits_{K_j} -\frac{\boldsymbol{r}-\boldsymbol{\xi}}{\left|\boldsymbol{r}-\boldsymbol{\xi}\right|^3} d\xi \right) dr \times \boldsymbol{\tau}_j^{(k)} = \boldsymbol{I}_{ij} \times \boldsymbol{\tau}_j^{(k)}, \quad k = 1,\, 2, \quad i,\, j = 1,\, \ldots,\, N.$$

Integral $\boldsymbol{I}_{ij}$ is calculated over triangular cells K_i and K_j, where i-th cell we call 'control', j-th cell — 'influence' cell.

The simplest way for integrals $\boldsymbol{I}_{ij}$, $i,\, j = 1,\, \ldots,\, N$, numerical computation is Gaussian quadrature formula usage. But this approach has high computational cost and leads to numerical calculation of improper integral when influence and control cells are neighboring (it means that they have common edge or common vertex).

The other way is to use some semi-analytical approaches. Firstly, the inner integral over the influence cell K_j can be calculated exactly:

$$\boldsymbol{J}_j(\boldsymbol{r}) = \int\limits_{K_j} -\frac{\boldsymbol{r}-\boldsymbol{\xi}}{\left|\boldsymbol{r}-\boldsymbol{\xi}\right|^3} d\xi. \tag{5.1}$$

Secondly, the outer integral over the control cell

$$\boldsymbol{I}_{ij} = \int\limits_{K_i} \boldsymbol{J}_j(\boldsymbol{r})\, dr \tag{5.2}$$

can be calculated using Gaussian dots in non-neighbor case. If the cells have common edge or common vertex, we need to exclude the singularity from the $\boldsymbol{J}_j(\boldsymbol{r})$ and write down it in form

$$\boldsymbol{J}_j(\boldsymbol{r}) = \boldsymbol{J}_j^{\,\mathrm{reg}}(\boldsymbol{r}) + \boldsymbol{J}_j^{\,\mathrm{sing}}(\boldsymbol{r}),$$

where $\boldsymbol{J}_j^{\,\mathrm{reg}}(\boldsymbol{r})$ has no singularities and can be easily integrated numerically with high accuracy, while the integral

$$\int\limits_{K_i} \boldsymbol{J}_j^{\,\mathrm{sing}}(\boldsymbol{r})\, dr$$

can be calculated exactly in analytic form.

There is well-known way for analytical calculation of integral (5.1) via considering of the integral from $\left|\boldsymbol{r}-\boldsymbol{\xi}\right|^{-1}$ with respect to $\boldsymbol{\xi}$ over the triangle K_j:

$$\boldsymbol{J}_j(\boldsymbol{r}) = \int\limits_{K_j} -\frac{\boldsymbol{r}-\boldsymbol{\xi}}{\left|\boldsymbol{r}-\boldsymbol{\xi}\right|^3} d\xi = -\int\limits_{K_j} \nabla_\xi \frac{1}{\left|\boldsymbol{r}-\boldsymbol{\xi}\right|} d\xi =$$

$$= \int\limits_{K_j} \nabla_r \frac{1}{\left|\boldsymbol{r}-\boldsymbol{\xi}\right|} d\xi = \nabla_r \left(\int\limits_{K_j} \frac{1}{\left|\boldsymbol{r}-\boldsymbol{\xi}\right|} d\xi \right).$$

The last integral is very usual in potential theory, analytical expression for it can be found, for example, in [7]. However, that expression is cumbersome and it also should be differentiated with respect to components of vector $\boldsymbol{r}$.

Using computational software of symbolic mathematics *Wolfram Mathematica* and Handbook of integrals [8] it is possible to integrate (5.1) straightforwardly if vectors $\boldsymbol{s}_k = \boldsymbol{r}_k^{(j)} - \boldsymbol{r}$, $k = 1, 2, 3$, are only known, where $\boldsymbol{r}$ is point for which integral (5.1) is calculated, $\boldsymbol{r}_k^{(j)}$ are position vectors for vertices of K_j triangular cell. Denoting

$$\boldsymbol{e}_k^{(j)} = \frac{\boldsymbol{s}_{k+1} - \boldsymbol{s}_k}{\left|\boldsymbol{s}_{k+1} - \boldsymbol{s}_k\right|} = \frac{\boldsymbol{r}_{k+1}^{(j)} - \boldsymbol{r}_k^{(j)}}{\left|\boldsymbol{r}_{k+1}^{(j)} - \boldsymbol{r}_k^{(j)}\right|}, \qquad \boldsymbol{\sigma}_k = \frac{\boldsymbol{s}_k}{\left|\boldsymbol{s}_k\right|}, \quad k = 1, 2, 3,$$

and assuming all the indices to be calculated using a modulus of 3, we obtain

$$\boldsymbol{J}_j(\boldsymbol{r}) = \Theta_j \boldsymbol{n}_j + \boldsymbol{\Psi}_j \times \boldsymbol{n}_j, \quad j = 1, \ldots, N;$$

where

$$\boldsymbol{\Psi}_j = \sum_{k=1}^{3} \ln\left(\frac{\left|\boldsymbol{s}_k\right|}{\left|\boldsymbol{s}_{k+1}\right|} \frac{1 + \boldsymbol{e}_k^{(j)} \cdot \boldsymbol{\sigma}_k}{1 + \boldsymbol{e}_k^{(j)} \cdot \boldsymbol{\sigma}_{k+1}} \right) \boldsymbol{e}_k,$$

Θ_j is signed solid angle subtended by triangular cell K_j which can be calculated, for example, by using the formula [9]

$$\Theta_j = 2 \arctan\left(\frac{\boldsymbol{s}_1 \boldsymbol{s}_2 \boldsymbol{s}_3}{\left|\boldsymbol{s}_1\right| \cdot \left|\boldsymbol{s}_2\right| \cdot \left|\boldsymbol{s}_3\right| + \left(\boldsymbol{s}_1 \cdot \boldsymbol{s}_2\right)\left|\boldsymbol{s}_3\right| + \left(\boldsymbol{s}_2 \cdot \boldsymbol{s}_3\right)\left|\boldsymbol{s}_1\right| + \left(\boldsymbol{s}_3 \cdot \boldsymbol{s}_1\right)\left|\boldsymbol{s}_2\right|} \right),$$

where $\boldsymbol{s}_1 \boldsymbol{s}_2 \boldsymbol{s}_3$ denotes the scalar triple product of the vectors.

The procedure of numerical calculation of the integral (5.2) depends on relative position of cells K_i and K_j. Three different cases should be considered: when the cells don't have common edges and vertices (non-neighbouring case), when cells have common edge (and two common vertices) and, finally, when they have common vertex only.

5.1. Non-neighbouring cells case. Calculation of the integral (5.2) when cells K_i and K_j don't have common edges and vertices, is provided numerically by using Gaussian quadrature formula:

$$\boldsymbol{I}_{ij} = \int_{K_i} \boldsymbol{J}_j(\boldsymbol{r})\, dr \approx A_i \sum_{p=1}^{N_{GP}} \omega_p \boldsymbol{J}_j(\boldsymbol{\eta}_p),$$

where N_{GP} is number of Gaussian points; ω_p are weight coefficients; $\boldsymbol{\eta}_p$ are positions of Gaussian points. Values of ω_p and $\boldsymbol{\eta}_p$ for different values of N_{GP} can be found, for example, in [10].

5.2. Neighbouring cells with common edge case. For simplicity we assume that all the cells are acute triangles, otherwise the numerical formulae should be modified and they becomes more complicated.

If cells K_i and K_j have common edge with directing unit vector $\boldsymbol{e}_c$, for example as it is shown on Fig. 5.1, we should apply Gaussian integration to regular part $\boldsymbol{J}_j^{\,\mathrm{reg}}(\boldsymbol{r})$, which has the form

$$\boldsymbol{J}_j^{\,\mathrm{reg}}(\boldsymbol{r}) = \boldsymbol{J}_j(\boldsymbol{r}) - \left(\boldsymbol{e}_1^{(j)} \ln\left(\frac{\boldsymbol{a} \cdot \boldsymbol{c}}{|\boldsymbol{c}|^2}\right) + \boldsymbol{e}_2^{(j)} \ln\left(-\frac{\boldsymbol{b} \cdot \boldsymbol{c}}{|\boldsymbol{c}|^2}\right) + \right.$$
$$\left. + \boldsymbol{e}_c \ln\left(\frac{|\boldsymbol{b}| \cdot |\boldsymbol{c}| + \boldsymbol{b} \cdot \boldsymbol{c}}{|\boldsymbol{a}| \cdot |\boldsymbol{c}| + \boldsymbol{a} \cdot \boldsymbol{c}}\right) \right) \times \boldsymbol{n}_j,$$

or, the same written down in the other way,

$$\boldsymbol{J}_j^{\,\mathrm{reg}}(\boldsymbol{r}) = \boldsymbol{J}_j(\boldsymbol{r}) - \left(\boldsymbol{e}_1^{\,(j)} \ln\Big(\frac{|\boldsymbol{a}\,|}{|\boldsymbol{c}\,|}\cos\alpha\Big) + \boldsymbol{e}_2^{\,(j)} \ln\Big(\frac{|\boldsymbol{b}\,|}{|\boldsymbol{c}\,|}\cos\beta\Big) + \right.$$
$$\left. + \boldsymbol{e}_c \ln\Big(\frac{|\boldsymbol{b}\,|(1-\cos\beta)}{|\boldsymbol{a}\,|(1+\cos\alpha)}\Big)\right) \times \boldsymbol{n}_j,$$

where $\boldsymbol{r}_1^{\,(j)}$ and $\boldsymbol{r}_3^{\,(j)}$ are position vectors of points $P_1^{\,(j)}$ and $P_3^{\,(j)}$, respectively;

$$\boldsymbol{e}_c = \frac{\boldsymbol{c}}{|\boldsymbol{c}\,|} = \boldsymbol{e}_3^{\,(j)}, \quad \boldsymbol{c} = \boldsymbol{r}_1^{\,(j)} - \boldsymbol{r}_3^{\,(j)}, \quad \boldsymbol{a} = \boldsymbol{r}_1^{\,(j)} - \boldsymbol{r}, \quad \boldsymbol{b} = \boldsymbol{r}_3^{\,(j)} - \boldsymbol{r},$$

$$\cos\alpha = \frac{\boldsymbol{a}\cdot\boldsymbol{c}}{|\boldsymbol{a}\,|\cdot|\boldsymbol{c}\,|}, \quad \cos\beta = -\frac{\boldsymbol{b}\cdot\boldsymbol{c}}{|\boldsymbol{b}\,|\cdot|\boldsymbol{c}\,|}.$$

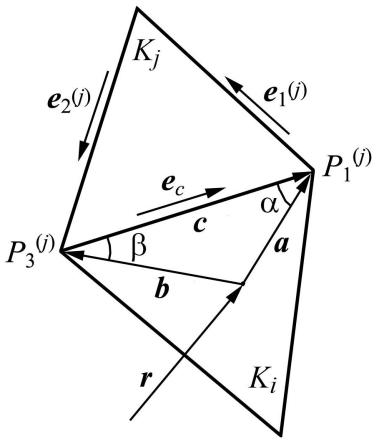

FIG. 5.1. *Cells K_i and K_j in case of having common edge*

Denoting

$$\boldsymbol{\Psi}_j^{\,\mathrm{sing}} = \boldsymbol{e}_1^{\,(j)} \ln\left(\frac{|\boldsymbol{a}\,|}{|\boldsymbol{c}\,|}\cos\alpha\right) + \boldsymbol{e}_2^{\,(j)} \ln\left(\frac{|\boldsymbol{b}\,|}{|\boldsymbol{c}\,|}\cos\beta\right) + \boldsymbol{e}_c \ln\left(\frac{|\boldsymbol{b}\,|(1-\cos\beta)}{|\boldsymbol{a}\,|(1+\cos\alpha)}\right), \tag{5.3}$$

we finally obtain

$$\boldsymbol{J}_j^{\,\mathrm{reg}}(\boldsymbol{r}) = \Theta_j \boldsymbol{n}_j + (\boldsymbol{\Psi}_j - \boldsymbol{\Psi}_j^{\,\mathrm{sing}}) \times \boldsymbol{n}_j, \quad \boldsymbol{J}_j^{\,\mathrm{sing}}(\boldsymbol{r}) = \boldsymbol{\Psi}_j^{\,\mathrm{sing}} \times \boldsymbol{n}_j.$$

All scalar multipliers in $\boldsymbol{\Psi}_j^{\,\mathrm{sing}}$ in (5.3) can be integrated analytically over the cell K_i:

$$q_1 = \int\limits_{K_i} \ln\left(\frac{|\boldsymbol{a}\,|}{|\boldsymbol{c}\,|}\cos\alpha\right) dr = -\frac{A_i}{2}\left(3 - 2\frac{\tan\beta_i}{\tan\alpha_i}\ln\left(1+\frac{\tan\alpha_i}{\tan\beta_i}\right)\right),$$

$$q_2 = \int\limits_{K_i} \ln\left(\frac{|\boldsymbol{b}\,|}{|\boldsymbol{c}\,|}\cos\beta\right) dr = -\frac{A_i}{2}\left(3 - 2\frac{\tan\alpha_i}{\tan\beta_i}\ln\left(1+\frac{\tan\beta_i}{\tan\alpha_i}\right)\right),$$

$$q_c = \int\limits_{K_i} \ln\left(\frac{|\boldsymbol{b}\,|(1-\cos\beta)}{|\boldsymbol{a}\,|(1+\cos\alpha)}\right) dr = A_i \ln\left(\tan\frac{\alpha_i}{2}\tan\frac{\beta_i}{2}\right) -$$
$$- \frac{|\boldsymbol{c}\,|^2}{2}\left(\sin\alpha_i \ln\left(\frac{|\boldsymbol{c}\,|^2\cos^2\left(\frac{\alpha_i}{2}\right)\sin\beta_i}{2A_i\cos^2\left(\frac{\alpha_i+\beta_i}{2}\right)}\right) + \sin\beta_i \ln\left(\frac{|\boldsymbol{c}\,|^2\cos^2\left(\frac{\beta_i}{2}\right)\sin\alpha_i}{2A_i\cos^2\left(\frac{\alpha_i+\beta_i}{2}\right)}\right)\right),$$

where α_i and β_i are angles of the triangle K_i, which adjoin the common edge of the cells K_i and K_j. Finally,

$$\boldsymbol{I}_{ij} = \int\limits_{K_i} \boldsymbol{J}_j^{\,\mathrm{reg}}(\boldsymbol{r})\,dr + \int\limits_{K_i} \boldsymbol{J}_j^{\,\mathrm{sing}}(\boldsymbol{r})\,dr \approx$$

$$\approx \left(A_i \sum_{p=1}^{N_{GP}} \omega_p \boldsymbol{J}_j^{\,\mathrm{reg}}(\boldsymbol{\eta}_p) \right) + \left(\boldsymbol{e}_c q_c + \boldsymbol{e}_1^{\,(j)} q_1 + \boldsymbol{e}_2^{\,(j)} q_2 \right) \times \boldsymbol{n}_j.$$

5.3. Neighbouring cells with common vertex case. If cells K_i and K_j have common vertex, for example as it is shown on Fig. 5.2, the regular part $\boldsymbol{J}_j^{\,\mathrm{reg}}(\boldsymbol{r})$ has the following form (the previous denotation is used):

$$\boldsymbol{J}_j^{\,\mathrm{reg}}(\boldsymbol{r}) = \boldsymbol{J}_j(\boldsymbol{r}) - \ln\left(\frac{|\boldsymbol{a}|}{\sqrt{A_j}} \right) \left(\boldsymbol{e}_1^{\,(j)} + \boldsymbol{e}_3^{\,(j)} \right) \times \boldsymbol{n}_j.$$

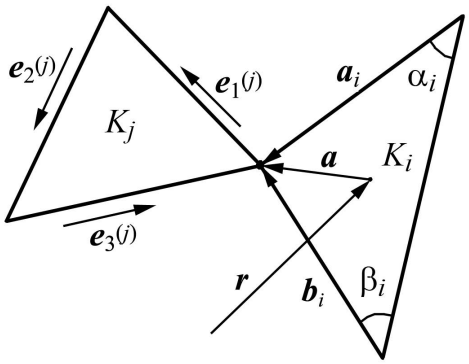

FIG. 5.2. *Cells K_i and K_j in case of having common vertex*

Again, denoting

$$\boldsymbol{\Psi}_j^{\,\mathrm{sing}} = \left(\boldsymbol{e}_1^{\,(j)} + \boldsymbol{e}_3^{\,(j)} \right) \ln\left(\frac{|\boldsymbol{a}\,|}{\sqrt{A_j}} \right), \tag{5.4}$$

we obtain

$$\boldsymbol{J}_j^{\,\mathrm{reg}}(\boldsymbol{r}) = \Theta_j \boldsymbol{n}_j + (\boldsymbol{\Psi}_j - \boldsymbol{\Psi}_j^{\,\mathrm{sing}}) \times \boldsymbol{n}_j, \quad \boldsymbol{J}_j^{\,\mathrm{sing}}(\boldsymbol{r}) = \boldsymbol{\Psi}_j^{\,\mathrm{sing}} \times \boldsymbol{n}_j.$$

The scalar multiplier in $\boldsymbol{\Psi}_j^{\,\mathrm{sing}}$ in (5.4) can be integrated analytically over the cell K_i:

$$q = \int\limits_{K_i} \ln\left(\frac{|\boldsymbol{a}\,|}{\sqrt{A_j}} \right) dr =$$

$$= \frac{1}{4} \left(2A_i \left(\ln\left(\frac{A_i}{A_j} \right) - 3 \right) + 2(\pi - \alpha_i - \beta_i) |\boldsymbol{a}_i| \cdot |\boldsymbol{b}_i| \sin\alpha_i \sin\beta_i + \right.$$

$$\left. + |\boldsymbol{a}_i|^2 \sin 2\alpha_i \ln\left(\frac{|\boldsymbol{a}_i|}{\sqrt{A_i}} \right) + |\boldsymbol{b}_i|^2 \sin 2\beta_i \ln\left(\frac{|\boldsymbol{b}_i|}{\sqrt{A_i}} \right) \right),$$

where α_i and β_i are angles of the triangle K_i, which don't adjoin the common vertex of the cells K_i and K_j. Finally,

$$\boldsymbol{I}_{ij} = \int\limits_{K_i} \boldsymbol{J}_j^{\mathrm{reg}}(\boldsymbol{r})dr + \int\limits_{K_i} \boldsymbol{J}_j^{\mathrm{sing}}(\boldsymbol{r})dr \approx \left(A_i \sum_{p=1}^{N_{GP}} \omega_p \boldsymbol{J}_j^{\mathrm{reg}}(\boldsymbol{\eta}_p) \right) + q \left(\boldsymbol{e}_1^{(j)} + \boldsymbol{e}_3^{(j)} \right) \times \boldsymbol{n}_j.$$

6. Numerical example. In order to estimate the error of the developed semi-analytical approach, when the singular part of the corresponding integrals is calculated analytically and the regular one is calculated numerically, the test problem of flow simulation around the sphere was considered. The surface of the sphere was triangulated, all the triangles were close to the regular ones. For numerical integration Gaussian quadrature formula was used with 13 points [10].

The results are compared with pure numerical approach, where the corresponding improper integrals are directly calculated numerically using the same numerical formula. The maximum and average values of relative error of $\boldsymbol{I}_{ij}$ computing for all pairs of cells with common edge and cells with common vertex are shown in Table 6.1, where

$$\delta \boldsymbol{I}_{ij} = \frac{|\boldsymbol{I}_{ij} - \boldsymbol{I}_{ij}^*|}{|\boldsymbol{I}_{ij}^*|} \cdot 100\,\%.$$

The exact (reference) solution $\boldsymbol{I}_{ij}^*$ was also computed numerically with high precision by using specific numerical methods, adapted for improper integrals computation, implemented in computer algebra system *Wolfram Mathematica*.

TABLE 6.1
Relative error $\delta \boldsymbol{I}_{ij}$ for cells with common edge and for cells with common vertex.

	Semi-analytical approach	Pure numerical approach
Cells with common edge		
Maximum error	0.25 %	95 %
Average error	0.07 %	12 %
Cells with common vertex		
Maximum error	0.07 %	15 %
Average error	0.05 %	1 %

The accuracy of integrals calculation is high enough to expect the high accuracy of the solution of the whole problem of vortex sheet intensity computation on the sphere. In the numerical experiment the sphere of the unit radius was considered, the surface triangular mesh was constructed by using Salome open-source software, uniform meshes consist of 106, 710 and 1305 triangle panels and non-uniform mesh with 320 panels were used.

The exact vortex layer intensity distribution $\boldsymbol{\gamma}^*$ over the sphere can be calculated by using analytical formulae, which can be found, for example, in [11].

The relative error is computed for the total vorticity over the panels:

$$\delta\Gamma = \max_i \frac{A_i|\boldsymbol{\gamma}_i - \boldsymbol{\gamma}_i^*|}{A_i|\gamma_i^*|} \cdot 100\,\%,$$

where A_i is area of i-th panel; $\boldsymbol{\gamma}_i$ — vortex sheet intensity on i-th panel, computed by using the developed algorithm (4.4) and the algorithm which corresponds to 'classical' approach with closed vortex frameworks and boundary condition for normal velocity components; $\boldsymbol{\gamma}_i^*$ — exact value of vortex sheet intensity at the center of i-th panel.

In Table 6.2 the results of performed numerical experiment are shown; h is average length of panels' edges.

TABLE 6.2
Relative error of total vorticity computing for the sphere with different surface meshes.

Number of panels N	Panels' edge size h	'Tangent' approach $\delta\Gamma_{tang}$	'Normal' approach $\delta\Gamma_{norm}$
106 (uniform)	0.25	5 %	20 %
320 (non-uniform)	0.05 . . . 0.31	10 %	80 %
710 (uniform)	0.10	1.3 %	15 %
1305 (uniform)	0.07	0.7 %	11 %

It is clear, that the developed approach allows to obtain much more accurate results in comparison with 'classical' approach, especially when the surface mesh is non-uniform.

7. Conclusion. The derived formulae for $\boldsymbol{I}_{ij}$ make it possible to construct numerical procedure for solving of the discrete analogue of the integral equation for vortex sheet intensity calculation in the framework of 'tangent' approach. These formulae usage allows to increase significantly the accuracy of vortex sheet intensity computation on bluff bodies surface. It allows to use arbitrary triangular mesh on body surface and to refine mesh near sharp edges, that is especially important for flow simulation around bodies with complicated geometry.

The analogue formulae can be easily obtained for vortex element upon boundary cells influence calculation as well as cells upon vortex element calculation, so the developed approach can be used for the vortex wake influence computation. It will make possible to implement this approach for unsteady 3D flow simulation around bluff bodies and improve significantly the accuracy of flow characteristics as well as hydrodynamic forces computation by using vortex methods.

REFERENCES

[1] G.-H. COTTET AND P.D. KOUMOUTSAKOS, *Vortex Methods: Theory and Practice*. CUP, 2000.
[2] I.K. MARCHEVSKY AND G.A. SHCHEGLOV, *3D vortex structures dynamics simulation using vortex fragmentons*, in ECCOMAS 2012, e-Book, Vienna (2012), pp. 5716–5735.
[3] S.N. KEMPKA, M.W. GLASS, J.S. PEERY AND J.H. STRICKLAND, *Accuracy considerations for implementing velocity boundary conditions in vorticity formulations*. SANDIA REPORT SAND96-0583, UC-700, 1996.
[4] K.S. KUZMINA AND I.K. MARCHEVSKY, *On Numerical Schemes in 2D Vortex Element Method for Flow Simulation Around Moving and Deformable Airfoils*, in Advanced Problems in Mechanics: Proceedings of the XLII School-Conference, St.Petersburg (2014), pp. 335–344.
[5] J.D. ANDERSON, *A history of aerodynamics*. Cambrige University Press, 1997.
[6] I.K. LIFANOV, L.N. POLTAVSKII AND G. VAINIKKO, *Hypersingular Integral Equations and Their Applications*, Chapman & Hall / CRC Press, Boca Raton, 2004.
[7] V.A. ANTONOV, I.I. NIKIFOROV AND K.V. KHOLSHEVNIKOV, *Elements of the theory of the gravitational potential, and some instances of its explicit expression*. St.-Petersburg University Press, 2008.
[8] I.S. GRADSHTEYN, I.M. RYZHIK, A. JEFFREY (ED.) AND D. ZWILLINGER (ED.), *Gradshteyn and Ryzhik's Table of Integrals, Series, and Products*. Elsevier, 2007.
[9] A. VAN OOSTEROM AND J. STRACKEE, *The Solid Angle of a Plane Triangle*. IEEE Trans. Biom. Eng. BME-30 (1983) **2**, pp. 125–126.
[10] O.C. ZIENKIEWICZ, R.L. TAYLOR AND J.Z. ZHU, *The Finite Element Method: Its Basis and Fundamentals*. Elsevier, 2013.
[11] L.M. MILNE-THOMSON, *Theoretical Hydrodynamics*. London, Macmillan & Co ltd, 1962.